



Cite this article: Bates KT, Savage R, Pataky TC, Morse SA, Webster E, Falkingham PL, Ren L, Qian Z, Collins D, Bennett MR, McClymont J, Crompton RH. 2013 Does footprint depth correlate with foot motion and pressure? *J R Soc Interface* 10: 20130009.
<http://dx.doi.org/10.1098/rsif.2013.0009>

Received: 7 January 2013

Accepted: 28 February 2013

Subject Areas:

biomechanics

Keywords:

foot pressure, footprint, locomotion, topological analysis, biomechanics, finite-element analysis

Author for correspondence:

K. T. Bates

e-mail: k.t.bates@liverpool.ac.uk

Electronic supplementary material is available at <http://dx.doi.org/10.1098/rsif.2013.0009> or via <http://rsif.royalsocietypublishing.org>.

Does footprint depth correlate with foot motion and pressure?

K. T. Bates¹, R. Savage¹, T. C. Pataky², S. A. Morse¹, E. Webster¹, P. L. Falkingham^{4,5}, L. Ren³, Z. Qian⁶, D. Collins¹, M. R. Bennett⁷, J. McClymont¹ and R. H. Crompton¹

¹Evolutionary Morphology and Biomechanics Research Group, Department of Musculoskeletal Biology, Institute of Aging and Chronic Disease, University of Liverpool, Sherrington Building, Ashton Street, Liverpool L69 3GE, UK

²Department of Bioengineering, Shinshu University, Nagano-ken, Ueda-shi 386-8567, Tokida 3-1-15, Japan

³School of Mechanical, Aerospace and Civil Engineering, University of Manchester, Pariser Building, PO Box 88, Manchester M60 1QD, UK

⁴Department of Comparative Biomedical Sciences, Structure and Motion Laboratory, Royal Veterinary College, London, UK

⁵Department of Ecology and Evolutionary Biology, Division of Biology and Medicine, Brown University, Providence, RI 02912, USA

⁶Key Laboratory of Bionic Engineering, Jilin University, Changchun 130022, People's Republic of China

⁷School of Applied Sciences, Bournemouth University, Talbot Campus, Fern Barrow, Poole, Dorset BH12 5BB, UK

Footprints are the most direct source of evidence about locomotor biomechanics in extinct vertebrates. One of the principal suppositions underpinning biomechanical inferences is that footprint geometry correlates with dynamic foot pressure, which, in turn, is linked with overall limb motion of the trackmaker. In this study, we perform the first quantitative test of this long-standing assumption, using topological statistical analysis of plantar pressures and experimental and computer-simulated footprints. In computer-simulated footprints, the relative distribution of depth differed from the distribution of both peak and pressure impulse in all simulations. Analysis of footprint samples with common loading inputs and similar depths reveals that only shallow footprints lack significant topological differences between depth and pressure distributions. Topological comparison of plantar pressures and experimental beach footprints demonstrates that geometry is highly dependent on overall print depth; deeper footprints are characterized by greater relative forefoot, and particularly toe, depth than shallow footprints. The highlighted difference between 'shallow' and 'deep' footprints clearly emphasizes the need to understand variation in foot mechanics across different degrees of substrate compliance. Overall, our results indicate that extreme caution is required when applying the 'depth equals pressure' paradigm to hominin footprints, and by extension, those of other extant and extinct tetrapods.

1. Introduction

Footprints are the most direct source of evidence about limb and foot biomechanics in extinct vertebrates [1–3]. Consequently, the fossil footprint record plays a central role in our understanding of locomotor evolution in many extinct and extant vertebrate groups, most notably hominins [1,2], dinosaurs [3,4] and the earliest terrestrial tetrapods [5]. In hominin palaeontology, in particular, footprints provide a crucial line of evidence for a number of key adaptive transitions in the evolutionary history of our own species, notably, the origin of modern fully erect bipedalism [1], and the functional transition in gait between early habitual bipeds such as *Australopithecus afarensis* and endurance walkers and runners such as early African *Homo erectus* [2].

One of the principal assumptions that underpins biomechanical inferences from footprints is that footprint topology—the three-dimensional surface relief of the deformed substrate—is directly indicative of dynamic foot pressure, which, in turn, is integrally linked with overall limb motion of the trackmaker

[1–4]. The same fundamental assumption is implicit in the study of modern forensic footprints [6,7], where three-dimensional footprint geometry (or metrics used to describe it) is considered diagnostic of specific individuals. A recent finding that foot pressures on hard or non-compliant surfaces are highly diagnostic of specific individuals [8] suggests that footprints may potentially represent powerful forensic tools, if a strong correlation between habitual motion, pressures and footprint depth can be quantitatively demonstrated.

However, currently, our quantitative understanding of locomotion and particularly foot biomechanics, in living vertebrates, is largely based on observations of movement on hard (non-compliant) substrates. The introduction of a compliant substrate adds a range of complexity that provokes a series of questions to which there are currently few answers; in particular, how is foot motion altered or mediated by substrate compliance? Furthermore, the extent to which foot motion and complex dynamically applied pressures are actually recorded in footprints remains poorly understood [9]. For example, how strongly does pressure correlate with depth and does it vary across the foot/footprint as substrate properties vary? Is footprint relief more indicative of maximal or time-integrated pressure? These questions remain pertinent and largely unanswered despite over 150 years of research [9,10], during which time experiments into the processes of footprint formation have failed to elucidate the complex relationships between sediment rheology and foot morphology, motion and pressures beyond the simplest level of inference (e.g. higher pressure equals deeper footprints; 'softer' sediment equals deeper footprints).

The aim of this study was to address these unanswered questions by quantitatively investigating the utility of footprints as indicators of habitual foot mechanics, so that their use in forensic and evolutionary studies may be appropriately constrained. We tackle this challenge by testing two specific null hypotheses: (HYP1) that the spatial distribution of pressure across the sediment surface during footprint formation is indistinguishable from the distribution of depth (three-dimensional topology) of the footprint; and (HYP2) that foot pressure topology on hard/non-compliant surfaces and footprint topology in compliant substrates are indistinguishable and therefore concepts of foot function established on hard substrates are directly applicable to footprints. That foot motion and pressure will vary according to substrate compliance may seem intuitive, and, indeed, one previous study identified relatively weak correlations between plantar pressures and footprints generated in sand [9]. However, in direct contrast, a very recent study [11] found significant correlations between measurements of plantar pressure and relative footprint depths at 10 anatomical regions across the foot, suggesting this issue remains poorly resolved.

To test these hypotheses, we carry out two novel experiments that integrate laboratory gait data, field experiments of locomotion in sand and computer simulations of human footprint formation. Specifically, we carry out computer-simulated indenter experiments to explore the relationship between pressure experienced by a compliant substrate and footprint geometry (i.e. depth) to address HYP1. In a second experiment, we conduct the first topological statistical comparison of human plantar pressure records from a non-compliant surface (a pressure sensing treadmill) and footprints generated in naturally deposited beach sand. This directly addresses HYP2 by constraining differences in foot function

between the two substrate types, and subsequently also tests the extent to which the distribution of plantar pressure recorded on hard surface correlates with footprint topology.

2. Material and methods

2.1. Data collection

2.1.1. HYP1: pressure–depth correlations in computer-simulated footprints

In order to directly investigate the relationship between pressure and footprint depth, we used a parametric computer modelling approach. Specifically, we modelled the dynamic interaction of a rigid human foot indenter with a compliant elastic–plastic substrate volume (figure 1) in the finite-element (FE) package ABAQUS (v. 6.9). The aim was not to model a specific substrate, but more to create a model in which a continuum of substrate strengths and loading conditions could be simulated. An elastic–plastic von Mises stress model was used to represent a clay- or mud-like cohesive substrate [12,13], defined by three parameters: shear strength (C_u), Poisson ratio (ν) and Young's modulus (E). Restricting the model to three basic inputs meant overall compliance could be easily manipulated, in concert with different loading inputs (see below), to examine pressure–depth relationships across a wide range of substrate strengths and applied pressures. A cohesive substrate model was chosen because we felt this substrate type offered the highest probability of supporting or rejecting HYP1. Excluding liquefaction failure in water-logged mud, failure mechanics are likely to be dominated by plastic deformation in cohesive substrates, with limited macro-scale shearing along failure surfaces [4]. As a consequence, we believe a simple elastic–plastic substrate model offers a best-case scenario for correlations between pressure and footprint depth, but accept restricting this analysis to cohesive substrates is a limitation in this study.

The substrate volume modelled had dimensions of length, width and depth of 1 m, which is equal to approximately 4.5 times foot length in all dimensions to avoid boundary effects [12,13]. The sediment volume was composed of 1 960 400 eight-node hexahedral elements, and in order to reduce element number (and consequently run time) while maintaining a high level of accuracy, a scaling algorithm was used that generated larger elements away from the area loaded beneath the foot. We derived a three-dimensional model of a human foot by segmenting the volume encapsulated by the skin outline (starting just above the ankle joint) from high-resolution micro-CT data using MIMICS (figure 1). The model was meshed in ABAQUS (150 338 tetrahedral elements) and treated as a rigid, non-deformable body in all analyses. Our simulations are therefore comparable to previous physical footprint indenter experiments [4] but provide considerable advantages by allowing absolute control and manipulation of simulation inputs (e.g. pressures, sediment properties) and the extraction of a wide range of output variables (e.g. pressure experienced across the substrate surface) not possible in physical modelling.

To investigate the relationship between foot kinetics, sediment rheology and footprint shape, we ran a variety of indentation simulations over a range of simulated substrate properties (see the electronic supplementary material, tables S1 and S2). Simulations fall into two major categories: those in which the substrate elements were given uniform properties, creating a homogeneous sediment volume, and those in which only a shallow surface layer of the sediment volume was given compliant material properties, with elements beneath given properties that can be considered stiff and incompressible, thereby mimicking the presence of a mechanically non-deformable sub-surface layer. In simulations with a completely homogeneous substrate mesh, deformation proceeds

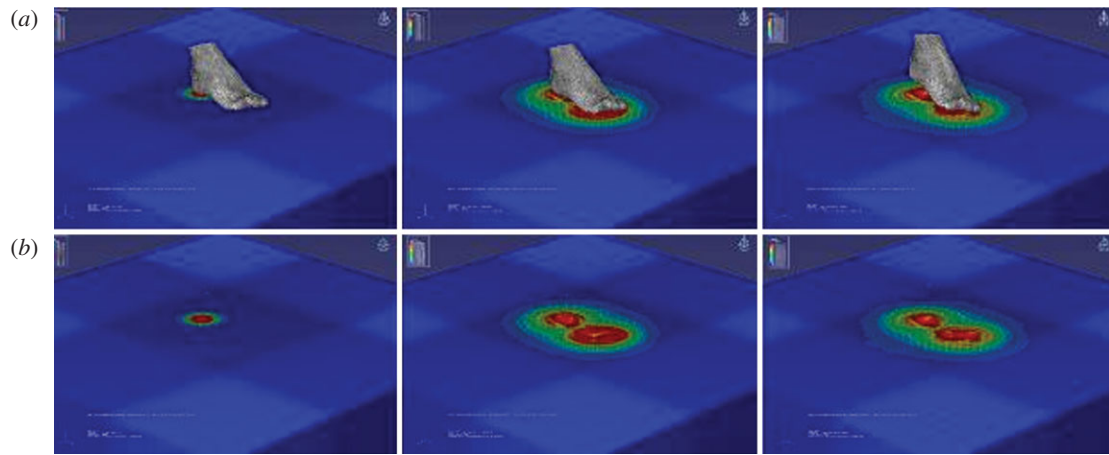


Figure 1. Snapshots from finite-element simulations showing three points during the indentation of the compliant cubic 'soil' mesh with a three-dimensional rigid foot indenter, (a) with and (b) without foot shown (soil mesh colour-coded with von Mises stress).

under the foot indenter until loading is artificially removed in the final simulation step, unless pressure is less than the bearing capacity, in which case no permanent (plastic) deformation would occur. Consequently, in these simulations, the substrate is unlikely to bear the load being applied in the manner that would have to occur during real locomotion in order to support body weight and allow re-acceleration to the next step without the track maker becoming mired. Simulations in a completely homogeneous substrate therefore isolate the effects of pure indentation and failure (related purely to foot shape and loading) on pressure–depth relationships. Additional of a firm sub-surface layer, able to support forces associated with foot loading, will subsequently highlight factors associated with substrate consolidation that impact on pressure–depth relationships.

Motion and loading of the foot was prescribed in two different ways. First, we conducted a series of simulations in which uniform negative pressures were applied to the heel and central forefoot regions (approximately the area surrounding the distal heads of metatarsals 2–4), thereby simulating a simple vertical indent into the soil mesh. In order to investigate more broadly realistic foot motions and pressures, we selected data for one individual from our treadmill foot pressure database (see below). Dynamic pressure of a single footfall with the lowest mean-squared error relative to that subject's overall mean peak pressure was simplified into six discrete time-intervals of equal duration. During each of the first five time-intervals, constant pressures were applied to the plantar surface of the foot model that were equal to the maxima of those experimentally recorded across the foot during that time interval. Specifically, within each time increment, the magnitude and distribution of pressure varied across regions of plantar surface approximated the actual variation across the foot recorded in experimental data (e.g. the initial increment had high heel pressures and no forefoot pressure; the final loading increment at toe-off had high forefoot pressure and no heel pressure), but was constant within each region of the foot throughout each time increment. This allowed relatively smooth transfer of pressure anteriorly across the plantar surface from the heel, along the lateral mid-foot and antero-medially across the metatarsal heads to the medial phalanges across the five-stepped increments. In the sixth time-interval, an upward displacement was applied to the foot so that it left the substrate, allowing any elastic recovery to occur in the substrate volume prior to termination of the simulation. Again, we emphasize that our aim was not to match treadmill motions and pressures precisely nor to produce footprints predictive of those of the experimental subject, but rather to investigate basic relationships between pressure, substrate strength and footprint depth distributions under conditions that are broadly representative of human walking. This initial pressure regime was

used as the starting point for a series of simulations in which we systematically varied foot pressure magnitude and distribution, loading duration, and substrate properties across large ranges of values (see the electronic supplementary material, tables S1 and S2).

2.1.2. HYP 2: comparing foot mechanics on non-compliant and compliant substrates

Experimental footprint analyses were conducted on a beach near New Brighton in the northwest of England on seven different days during 2011. The use of naturally deposited sediment is critical allowing extended trails and avoiding issues of artificial sediment packing which results when using laboratory-based sand trays. Ten subjects in total participated in the experiments, with different combinations of subjects present on different days (see the electronic supplementary material, table S3).

On each day, subjects wore reflective tape on their hips, knees, ankles and distal feet, and were asked to walk barefoot along the beach perpendicular to a high-definition video camera mounted on a tripod (see the electronic supplementary material, figure S1). Subjects were asked to walk at a natural walking speed until they had made approximately 20 consecutive footprints. Average walking speeds calculated from the reflective markers ranged from 1.08 to 1.27 m s⁻¹ (overall mean 1.17 m s⁻¹ ± 0.06 s.d.). All subjects made their footprints within the same 5-min period on any given day to minimize differences in sediment rheology owing to temporal changes in moisture content. All footprints made in undisturbed sediment were then digitized using either a high-resolution laser scanner (NextEngine three-dimensional scanner HD) or the photogrammetric approach of Falkingham [14]. Both methods provided digital models of resolution in excess of that required for our pixel-level topographic analysis [14] and were down-sampled to 1 mm resolution at the pre-analysis stage (see below). In total, 358 footprints were digitized (see the electronic supplementary material, table S3).

The same 10 subjects that participated in the beach experiments walked barefoot at a constant speed of 1.1 m s⁻¹ (within range of beach speeds, see above and electronic supplementary material, figure S2) on a Zebris FDM-THM foot pressure sensing treadmill for approximately 10 min, with dynamic pressures recorded at a frequency of 100 Hz. The treadmill was set to a zero incline. During this period, pressure data were collected for 10 intervals of 30 s. We synchronously collected kinematic data using an integrated 12-camera Qualysis motion capture system, with an array of 27 spherical markers across the body that included the six hindlimb markers used in the beach trials. For each step recorded, pressure data corresponding to the maximum pressure and pressure–time (PT) integral recorded

across the foot during were extracted using a custom program. This yielded between 454 and 519 pedobarographic records for the 10 individuals (see the electronic supplementary material, table S4).

2.2. Data analysis

In order to quantitatively compare three-dimensional footprint form, we used pedobarographic statistical parametric mapping (pSPM), a topological technique recently adapted for foot pressure [15,16] and footprint studies [1]. This technique allowed us to carry out statistical pixel-by-pixel, or element-by-element comparison of different footprints, plantar pressure records and FE simulation outputs, to quantitatively and objectively compare pressure at the substrate–foot interface and footprint depth. As a statistical approach, pSPM presents a number of benefits for footprint analyses (see [1] for discussion). Principally, it is not susceptible to problems of ad hoc or subjective region of interest discretization, and its ability to assess the entire spatial domain of the footprints, allowing objective statistical comparisons and inferences to be made on multiple records rather than individual prints.

All image processing and analysis were conducted using MATLAB (MathWorks, USA). For pressure records and experimental footprints, images were registered within each subject using an algorithm that minimized the mean-squared error between the images [15,16] such that homologous structures optimally overlapped. The same procedure was used to carry out topological comparisons of footprint depth and pressure characteristics in the FE simulations, using three-dimensional nodal positions and contact pressures experienced during the simulations by the surface nodes of the substrate mesh. To generate samples of FE models for comparison, we grouped simulations in which foot loading characteristics were constant but sediment properties varied. We also created subsamples based on depth in order to compare pressure–depth relationships in shallower versus deeper prints (cut-off corresponding to the mean of the maximum depths of all simulations). In order to compare depth and pressure, all records were normalized by their maximum value (depth or pressure).

3. Results

3.1. HYP1: pressures versus depths in computer-simulated footprints

The spatial distribution of depth differed from the distribution of both peak pressure and pressure impulse in each individual FE simulation (figure 2). When prints were combined into populations based on common loading inputs and overall depths, the mean of each grouping displayed large differences between relative depth and both peak and time-integral of pressure (figure 2*a–f*). In all simulations, pressure was relatively greater than depth under the forefoot (metatarsal heads), whereas relative heel depth tended to exceed relative pressure, particularly in simulations with the firm sub-surface layer present (figure 2*e,f*). When simulations are grouped by depth, these same qualitative relationships between pressure and depth remain, but with notable variation in the magnitude of this difference (figure 2*g–j*). In ‘deep’ simulations without a mechanically firm sub-surface layer, relative pressure greatly exceeded depth across the entire print, except under the heel where depth exceeded pressure (figure 2*h*). Addition of the mechanically firm sub-surface layer reduced the magnitude of disparity under the forefoot, whereas pressure–depth differences under the heel became greater

(figure 2*j*). The same topological differences are present in shallow simulations, but the magnitude of disparity is greatly reduced, particularly in simulations with a mechanically firm sub-surface layer present (figure 2*i*).

3.2. HYP2: plantar pressures versus beach footprint topology

Figure 3 shows the mean beach footprint and mean peak plantar pressure record for each individual, alongside the SPM showing areas of major difference and associated levels of statistical significance (p -values) based on the two datasets. Figure 4 shows the same information for beach footprints compared with the PT integral recorded in the treadmill experiments.

Trends are evident in the comparisons in figures 3 and 4, despite considerable intra-subject variation in both footprint and plantar pressure topology. In particular, statistically significant differences between treadmill pressures and beach footprint topology are concentrated at the posterior (heel) and anterior (toes) areas of the records (figures 3 and 4). There are generally no statistically significant differences in mid- and posterior-forefoot topology, although some individuals do display some differences in the rear part of the forefoot (figures 3*e,g,i* and 4*e,g,i*).

Figure 5 shows a comparison of treadmill peak pressures with beach footprints for the subject that recorded the largest number of footprints, with the footprints split into subpopulations based on maximum depth. The general pattern observed for this subject is reflected in almost all individuals, and when the same footprint subpopulations are compared with PT integrals (see the electronic supplementary material, figures S3–S22). Shallow footprints (less than 20 mm max depth) generally show fewer or less widespread statistically significant topological differences to foot pressure topology, and SPMs are characterized by relatively deeper toe impressions but shallower impressions under the metatarsal heads than would be predicted from foot pressure records (figure 5 and electronic supplementary material, S3–S22). Statistically significant differences observed in the heel of shallower footprints and pressure records are generally also present in deeper footprints, despite a notable increase in disparity in forefoot and toe depth versus pressure. Specifically, SPMs of deep footprints (more than 20 mm max depth) versus pressure records show much greater differences in the forefoot region, with relative footprint depth exceeding pressure magnitude in all individuals (figure 5 and electronic supplementary material, S3–S22).

4. Discussion

4.1. HYP1: correlating foot pressure and footprint depth

By allowing precise manipulation of system parameters and direct comparison of results, our FE simulations highlight the basic causal mechanisms underpinning the pressure–depth relationship in the modelled compliant medium, representative of generic cohesive clay- or mud-like substrates. Previous indenter experiments [4,13,14] have largely focused on sediment failure during track formation, but it is clear from our results that understanding the consolidation and ultimate resistance of the substrate to dynamic loading after initial

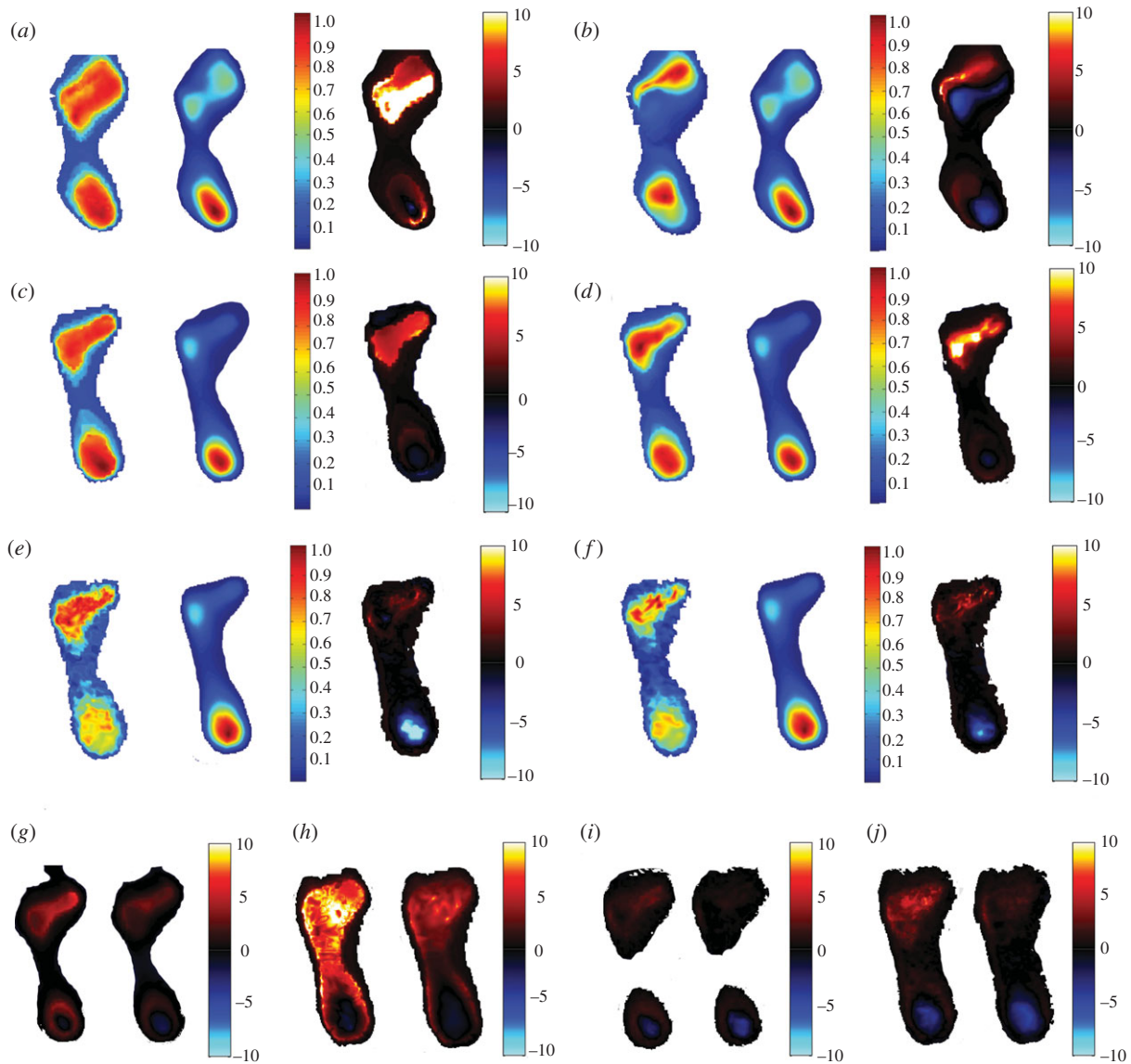


Figure 2. Exemplar results from finite-element simulations. Topological comparisons of the means (*a*) peak pressure and (*b*) PT integral to depth with uniform, vertical loading inputs and a homogeneous substrate mesh. Topological comparisons of the means (*c*) peak pressure and (*d*) PT integral to depth with initial dynamic loading inputs and a homogeneous substrate mesh. (*e,f*) Equivalent topological comparisons of means for the same loading inputs but with a firm sub-surface layer present in the substrate mesh. In (*a–f*), images from left to right are the mean pressure, mean depth and difference maps. (*g–j*) Difference maps between mean pressure and depth in populations ‘shallow’ and ‘deep’ computer-simulated footprints (*g,h*) without and (*i,j*) with the firm sub-surface layer. In (*g–j*), comparisons of peak pressure and depth are on the left, and PT integral and depth on the right. In difference maps, red show areas in which pressure is relatively greater than depth, whereas blue areas depict where depth exceeds pressure.

failure is also critical to understanding pressure–depth correlations in footprints.

Simulations in a completely homogeneous substrate isolate the effects of pure indentation and failure (related purely to foot shape and loading) on pressure–depth relationships. That the same qualitative disparity between pressure and depth is found in these simulations, regardless of whether pressures are applied uniformly across the foot in a subvertical indentation (figure 2*a,b*), or in a non-uniform pattern mimicking treadmill pressures (figure 2*c,d,g,h*), strongly suggests that discrete regions of the plantar foot differ in their indentation potential. Falkingham *et al.* [12] demonstrated that indenter shape, specifically the ratio of edge length to surface area, influences penetration depth in compliant media. The mismatch between the relative distribution of pressure and depth in our simulations is consistent with the shape effects described by Falkingham *et al.* [12]. In cohesive substrates, shapes with

relatively less edge length penetrate to greater depths for a given pressure [12]. The sub-circular, highly curved shape of the heel provides a relatively low edge length to surface area compared with the sub-rectangular, relatively flat shape of the forefoot, helping to explain the relative disparity between pressures and depths under the heel and forefoot in our simulations (figure 2).

Introduction of a mechanically firm sub-surface layer at shallow depth modifies the pressure–depth relationship observed in simulations with a homogeneous substrate mesh (figure 2). Specifically, areas in which pressure exceeds depth become restricted to small or localized areas under the forefoot, while under the heel disparity increases (i.e. depth > pressure) throughout the simulations (figure 2). This change is the direct result of the ability of the firm sub-surface layer to absorb the load applied by the moving indenter without deforming, resulting in a redistribution of stress and strain in the compliant surface

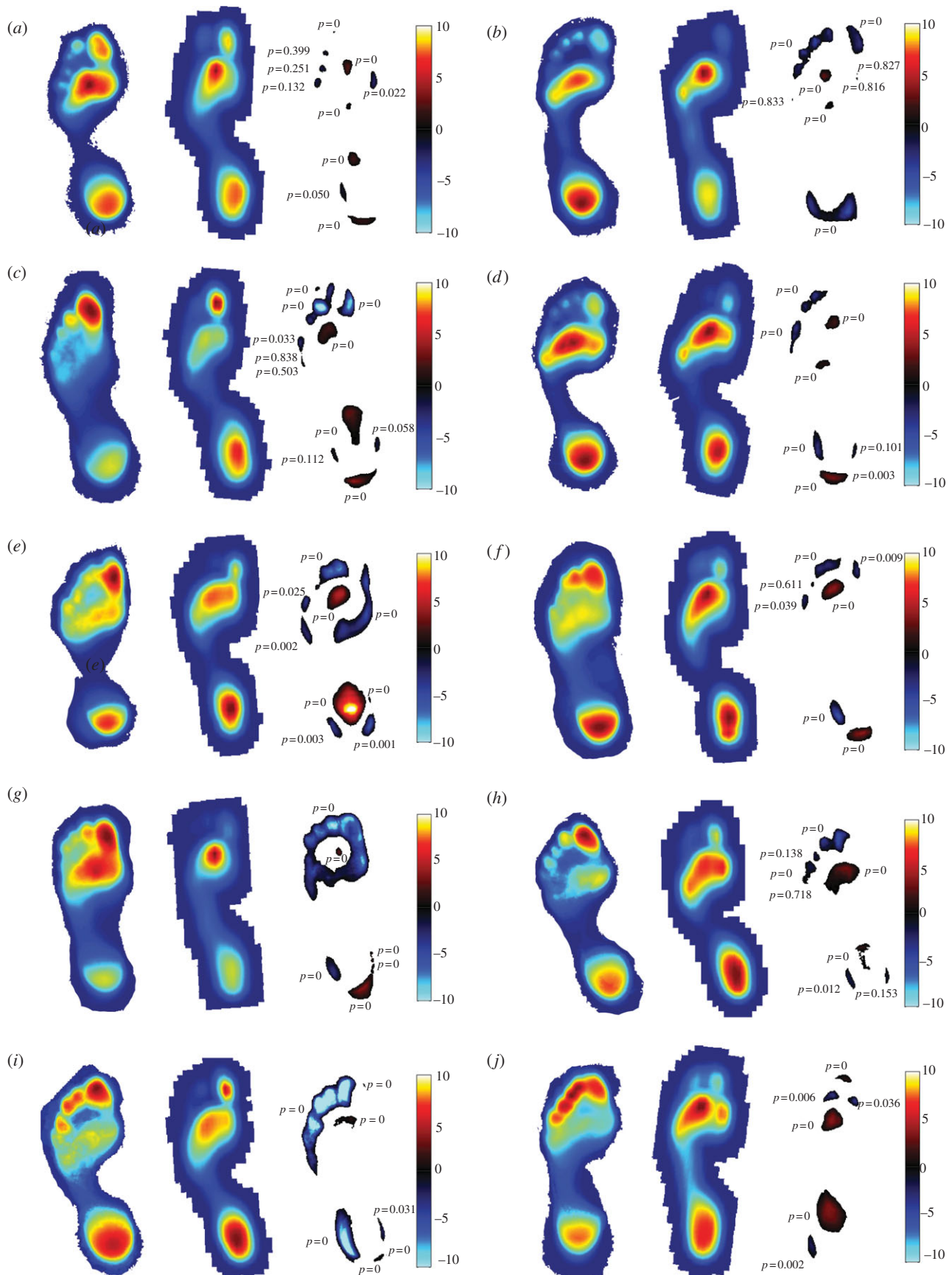


Figure 3. Topological comparisons of beach footprint depth and peak plantar pressure during treadmill walking in 10 subjects (*a–j*). Images shown are (left) mean beach footprint (centre) mean peak plantar pressure and (right) statistical parametric maps showing areas of difference and levels of statistical significance. In mean depth and pressure images, darker reds are higher values and blues lower values (depths/pressures), whereas in SPMs blue areas indicate relatively higher depths in footprints and reds relatively higher values in pressure records.

layer. This alters not only the depths of simulated footprints (e.g. the maximum decrease observed was 3.18 mm or 16.3%) but also the absolute values and the relative distribution of pressure

occurring during the simulations (figure 2*b*). In particular, relative pressure under the heel is reduced, and the highest pressures occur instead beneath the forefoot (figure 2*a–d*).

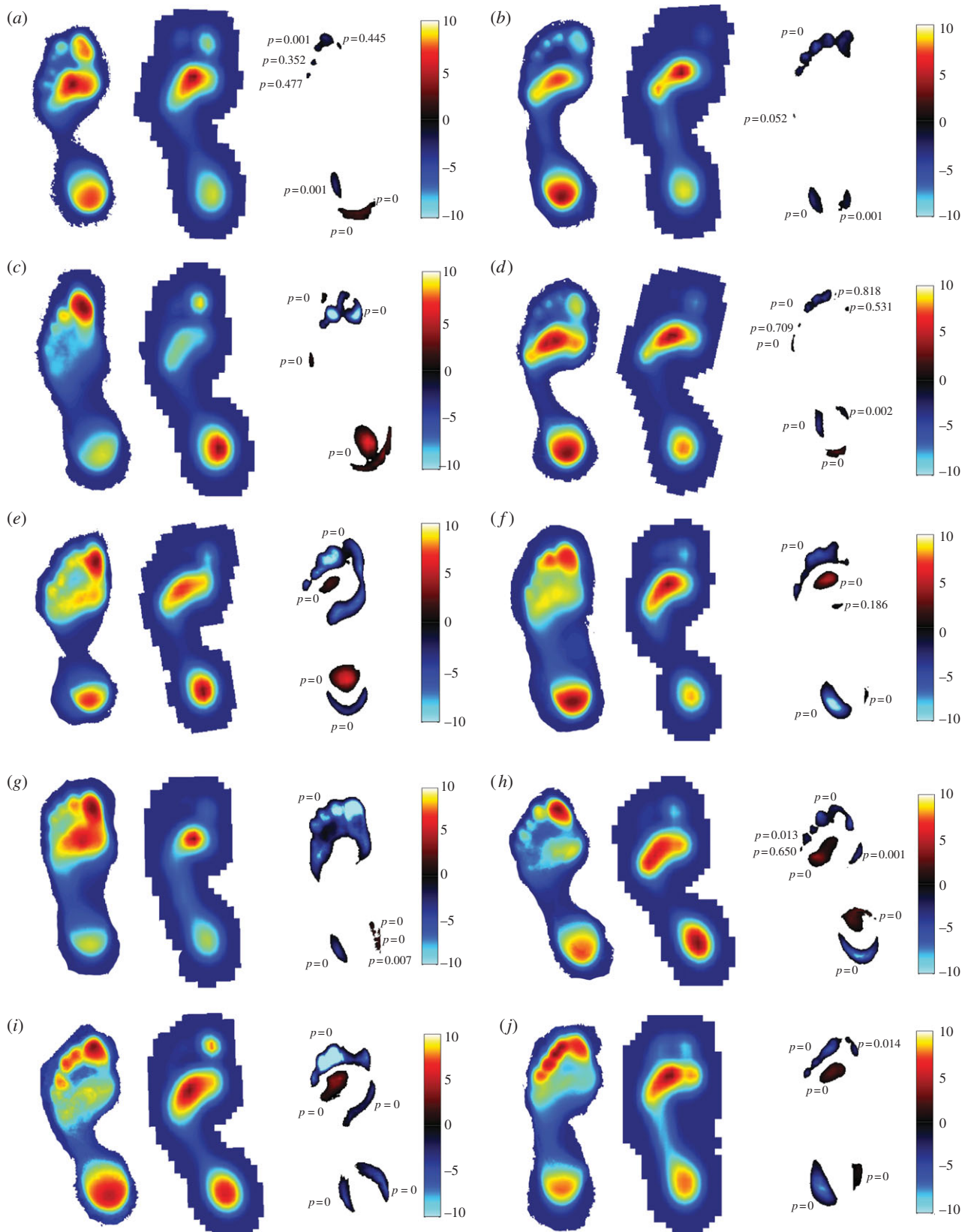


Figure 4. Topological comparisons of beach footprint depth and PT integral of plantar pressure during treadmill walking in 10 subjects (*a–j*). Images shown are (left) mean beach footprint, (centre) mean PT integral of plantar pressure and (right) statistical parametric maps showing areas of difference and levels of statistical significance. In mean depth and pressure images, darker reds are higher values and blues lower values (depths/pressures), whereas in SPMs blue areas indicate relatively higher depths in footprints and reds relatively higher values in pressure records.

This occurs because penetration of the posterior foot ceases as maximum compaction of the compliant surface layer beneath it is reached and consequently, with loading under the heel supported, the rigid indenter is able to roll or pivot forward and exert relatively higher pressure under the forefoot.

Thus, with respect to HYP1, objective topological comparisons between pressure and depth at the foot–sediment interface suggest that footprint depth is a poor predictor of pressure across a wide range of substrate strengths and loading regimes. Simulations suggest that only analyses of

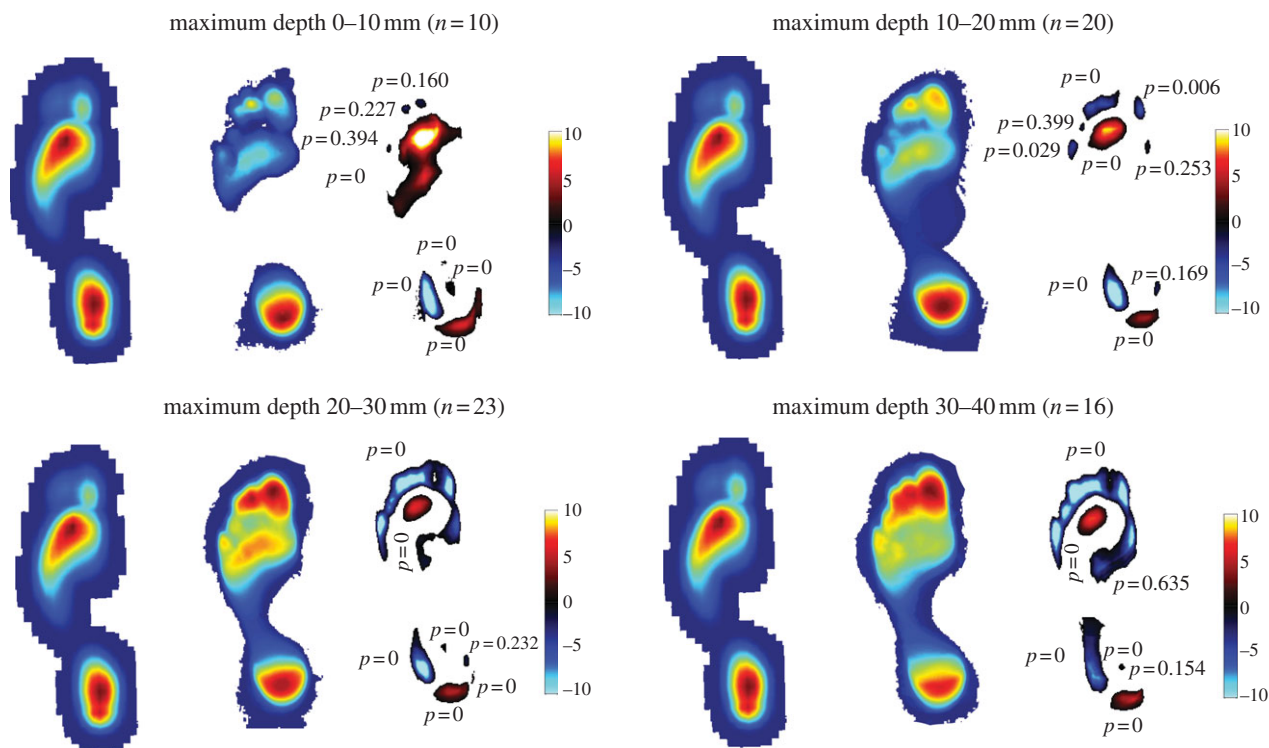


Figure 5. Topological comparisons of beach footprint depth and peak plantar pressure during treadmill walking in subject 6, with beach footprints split into subpopulations based maximum depth. Images shown are (left) overall mean peak plantar pressure, (centre) mean beach footprint for the subpopulation and (right) statistical parametric maps showing areas of difference and levels of statistical significance.

shallow footprint populations—in which confounding factors associated with foot–sediment interaction are reduced relative to deep prints—may yield reliable information on foot motion and pressures of the trackmaker. As footprint depth increases, our simulations suggest inferences about foot motion, and pressure derived from footprint geometry become less reliable (figure 2).

The relatively poor correlation between pressure and depth in our simulations is perhaps even more concerning given the simplicity of both our substrate and foot models. Here, we have modelled a relatively simple compliant substrate, excluding physical heterogeneity (e.g. vertical grading of sediment properties such as grain size, sorting and moisture content) and importantly more complex mechanical properties and behaviours often thought to occur in footprint formation (e.g. large-scale shear failure, liquefaction [4]). Furthermore, modelling the foot as a rigid body excludes more complex ground contact patterns and pressure distributions resulting from plantar and/or dorsiflexion, which may be negligible in the hind- and mid-foot but is almost certain significant in the fore-foot, particularly at the metatarsophalangeal joints (see §4). It seems likely that increased complexity in the substrate and foot models would introduce further mechanisms or potential for worsening the correlation between pressure and footprint depth. Our simulations strongly suggest that without extended mechanistic understanding, hypotheses about foot mechanics drawn from the assumption of strong pressure–depth correlations in footprints may be open to significant error (figure 2).

4.2. HYP2: foot function on compliant versus non-compliant substrates

The relatively minor, statistically significant differences between normalized topology of plantar pressures and shallow

beach footprints (less than 20 mm max depth; figure 5 and electronic supplementary material, S3–S22) suggest relatively modest differences in foot motion (and by inference, internal forces) across the two substrate types. Pressure records show that heel and forefoot pressures (typically under the metatarsal heads) are approximately equal on non-compliant surfaces, whereas in shallow footprints, forefoot impressions are shallower than the heel (figure 5 and electronic supplementary material, S3–S22). This distinction leads to significantly greater forefoot pressure values (peak and PT-integral) relative to depth in shallow footprints (figure 5 and electronic supplementary material, S3–S22), mimicking the difference seen in the FE simulations despite the difference in substrate properties (figure 2). Statistically significant differences at the heel are largely a function of sediment compression/deformation and three-dimensional footprint shape rather than disparity in pressure–depth related to foot function. In plantar pressure records, the high-pressure zone under the heel is relatively long and narrow, mimicking actual heel shape in the subjects. By contrast, in footprints, sediment is displaced medially and laterally about the heel, and on occasion uplifted posteriorly, to produce an impression with a more shortened and more rounded heel than in plantar pressure records (figures 3–5). Shallow depths under the metatarsal heads in beach footprints relative to pressures measured on the treadmill may result from the same shape mechanism by which the same difference occurs in the computer-simulated footprints. The experimental prints were made in a non-cohesive (sandy) substrate, but shallow prints show no evidence of internal shear failure and their shallow, smooth topology appears indicative of formation through pure compression and consolidation beneath the foot. It is possible that greater toe depths relative to plantar pressures are representative of the greater use of toes in propulsion through

flexion–extension of metatarsophalangeal joints, but given the shallow absolute depths, it is perhaps more likely that toes indent non-cohesive sediment more effectively than does the posterior-forefoot.

It might be expected that shallow footprints would show at least reasonable topological consistency with plantar pressure records, and that they should show lesser differences than deeper footprints given the increased capacity for divergence created by greater substrate deformation. However, our topological analysis suggests a clear distinction between footprints of less than 20 mm versus more than 20 mm depth, and the nature of this distinction strongly suggests a difference in foot forces and motion. Deeper footprints maintain topological differences under the heel that are likely attributable to substrate deformation and foot shape rather than to foot mechanics. This suggests little pre-conditioning of the foot, or active response during heel-down in footprint formation (whether shallow or deep) compared with on the non-compliant treadmill surface. However, in all subjects studied here, deeper footprints were characterized by relatively greater forefoot depths, which reverses the nature of the statistically significant difference between depth and forefoot pressure observed in shallow prints. Specifically, relative forefoot depth in deep footprints exceeds relative pressure measured on a non-compliant substrate (figure 5 and electronic supplementary material, S3–22).

We propose that relatively deeper forefoot impressions indicate a modified response of the mid- and forefoot to different external mechanical demands. Deeper prints reflect greater substrate compliance (i.e. lower bearing capacity), and the impression of the heel to greater depth will result in exaggerated deceleration of the foot and energy loss as work is done to displace sediment. Accordingly, substantial propulsion will be required from mid-stance onwards, to reaccelerate and vault the centre of mass forward over the standing foot. In turn, this is likely to increase pressure under the forefoot, associated with increased dorsiflexion at the metatarsophalangeal joints, as suggested by the large relative increase in toe depths (figure 5 and electronic supplementary material, S3–S22). Increased dorsiflexion moments at the metatarsophalangeal joints will place increased demands on extrinsic and intrinsic digital flexors, which will also be contracting eccentrically to control and to assist ankle plantar flexors in generating acceleration into the swing phase.

LeJeune *et al.* [17] found that walking over sand incurred a 2.1–2.7-fold increase in the metabolic cost of locomotion versus a non-compliant surface, primarily owing to an increase in muscle–tendon work associated with ‘awkward limb movements’ in sand. Our topological statistical analysis of foot pressures and footprint depths elaborates on the kinematic and kinetic mechanisms underpinning the difference in foot mechanics on compliant versus non-compliant surfaces inferred by LeJeune *et al.* [17]. The increased cost of locomotion on sand they observed may be largely due to the need to overcome the earlier-discussed deceleration, and the greater muscle–tendon forces required to generate propulsion through increased forefoot motion.

Our depth-related trends may be comparable to the results of a kinematic and ground reaction force analysis of horses trotting in ‘firm wet’ versus ‘deep wet’ beach sand [18]. This analysis showed that while maximal ground reaction force decreased in deep wet sand (due primarily to

increased stance duration), the propulsive phase of stance was both longer and the corresponding impulse higher [18]. While the rigid hoof of horses obviously bears little resemblance to the human foot, the basic kinetic mechanisms of interaction between a moving limb and compliant substrate appear to be comparable in this context.

Our results emphasize the strong depth-dependent nature of footprint geometry, indicating (HYP2) that foot motion and pressure varies significantly according to the level of substrate compliance. The influence of footprint depth on relative geometry (and by inference foot motion) has been largely neglected in biomechanical interpretations of footprints. For example, without explicitly controlling for absolute depth, Raichlen *et al.* [19] suggested that similarity in the ratio of point depths from the heel and forefoot region of the Laetoli fossil footprints to those of an experimental dataset of humans indicated ‘modern’ upright walking in the 3.66 Ma trackmaker. Similarly, it has been argued that footprints made by primitive non-avian theropod dinosaurs using predominantly ‘hip-based’ limb retraction would have proportionally deeper heel impressions than those made by more derived avian (or ‘avian-like’) theropods in which limb retraction is predominantly ‘knee-based’ [4]. Clearly, future analyses that attempt to test such hypotheses must account for the potential for strong depth-dependency in footprint geometry and the specific role of substrate compliance in controlling the dynamics of the foot and propulsion (figures 5 and electronic supplementary material, S3–S22).

4.3. Comparison with previous work

We are aware of one previous attempt to quantitatively test the correlation between the relative distribution of plantar pressure and footprint depth [9]. Direct comparison of FE results to this previous experimental work is difficult owing to difference in the sediment types and respective analytical approaches. To examine pressure–depth correlations within footprints, D’Aout *et al.* [9] measured pressure at depth beneath the sediment surface in sand (non-cohesive), whereas we compared pressure and depth at substrate–foot interface directly in our cohesive substrate models (figure 2). Furthermore, this previous work used a subsampling, region of interest approach in which single point measurements were used to represent depths and pressures from discretized regions of pressure records and footprints. It has been shown that such subsampling may conflate pressure differences evident in pixel-level data, obscuring or even reversing statistical trends when compared with a more comprehensive topological analysis of multiple, whole plantar pressure [15,16] and depth records [1], as used here.

These differences mean we can only make broad qualitative comparisons of our beach footprint and plantar pressure analysis with previous studies. D’Aout *et al.* [9] and Hatala *et al.* [11] used similar experimental and statistical approaches to examine the correlation between pressure recorded on a non-compliant surface (a pressure plate) and footprint depth in a compliant substrate. As noted earlier, differences in sediment types and particularly statistical approaches make direct quantitative comparisons with these studies less than straightforward, but clearly our finding of systematic, statistically significant differences between peak and time-integral plantar pressure and footprint depth in sand is qualitatively more similar to the results of D’Aout *et al.* [9]. In contrast to the significant

correlations found across the foot by Hatala *et al.* [11], D'Aout *et al.* [9] found only weak-to-moderate statistical correlations between footprint depth and peak plantar pressure at the 'heel zone' and fifth metatarsal; and in the heel and mid-foot, when depth was compared with the PT integral. Because neither study performed any independent analysis of footprints of different depths, it is possible that levels of correlation were influenced by juxtaposing trends in shallower versus deeper footprints (figure 5). In contrast to D'Aout *et al.* [9], we find little difference in the predictive power of peak pressure and the PT integral (figures 2–5 and electronic supplementary material, S3–22). D'Aout *et al.* [9] suggested that peak pressure is the best predictor of depth in the heel but that impulse gains more importance distally. However, our FE and treadmill peak and PT integral records have similar topologies. Hence, when analysed topologically, both peak and PT integral records are equally predictive (or non-predictive) of footprint depth (figures 2–5 and electronic supplementary material, S3–22; but see figure 2*a,b*).

5. Conclusions

The assumption that footprint depth correlates closely with the distribution of pressure dynamically applied by the trackmaker's foot during print formation is the fundamental basis on which use of footprints in studies of forensics [6–7] and evolutionary biomechanics [1–4,9,19] can be justified. However, results from our modelling and experimental approaches suggest that a degree of caution should be exercised when applying this paradigm to human (or hominin) footprints, and by extension, to those of other extant and extinct tetrapods.

Our simple parametric FE model demonstrates the importance of understanding not only sediment failure and foot penetration but also underfoot substrate consolidation during print formation. Here, we have modelled the presence of a mechanical firm sub-surface layer and its impact on pressure–depth relationships in footprints. However, this interaction is just one of many possible factors that may allow the

sediment to resist deformation under load and support pressures associated with a trackmaker's locomotion. There is clearly a great need to extend the current level of physical and computational modelling of footprint formation to include factors such as mechanically distinct sub-surface layers and vertical grading of sediment properties such as grain size, sorting and moisture content, in order to better understand their impact on pressure–depth correlations. Given that we have modelled a relatively simple compliant substrate, excluding more complex mechanical properties and behaviours often thought to occur in footprint formation (e.g. large-scale shear failure, liquefaction [4]), our results suggest that without this extended mechanistic understanding, hypotheses about foot mechanics drawn from the assumption of strong pressure–depth correlations in footprints may be open to significant error (figure 2).

Our novel topological comparison of plantar pressure records and beach footprints demonstrates that footprint geometry is highly depth-dependent; deep footprints (more than 20 mm maximum depth) retain the relatively deep heel impressions present in shallow footprints (less than 20 mm maximum depth) but are characterized by greater relative forefoot, and particularly toe, depth (figure 5 and electronic supplementary material, S3–S22). The highlighted difference between 'shallow' and 'deep' footprints clearly emphasizes the need to understand variation in foot mechanics across different degrees of substrate compliance, as well as considering the depth-dependency of footprint geometry when comparing footprints from different sediment types and spatio-temporal locations before constructing higher-level biomechanical hypotheses.

This research was supported by a grant to R.H.C. and M.R.B from the Natural Environmental Research Council, UK (NE/H004246/1), and further supported by the MRC and Arthritis Research UK as part of the MRC–Arthritis Research UK Centre for Integrated Research into Musculoskeletal Ageing (CIMA). All procedures were approved by the University of Liverpool Research Ethics Committee (RETH 0000888). Cliff Addison is thanked for access to the University of Liverpool's HPC facilities.

References

- Crompton RH, Pataky TC, Savage R, D'Aout K, Bennett MR, Day MH, Bates K, Morse S, Sellers WI. 2012 Human-like external function of the foot, and fully upright gait, confirmed in the 3.66 million year old *Laetoli hominin* footprints by topographic statistics, experimental footprint-formation and computer simulation. *J. R. Soc. Interface* **9**, 707–719. (doi:10.1098/rsif.2011.0258)
- Bennett MR *et al.* 2009 Early hominin foot morphology based on 1.5-million-year-old footprints from Ileret, Kenya. *Science* **323**, 1197–1201. (doi:10.1126/science.1168132)
- Gates SM, Middleton KM, Jenkins Jr FA, Shubin NH. 1999 Three dimensional preservation of foot movements in Triassic theropod dinosaurs. *Nature* **399**, 141–144. (doi:10.1038/20167)
- Manning PL. 2004 A new approach to the analysis and interpretation of tracks: examples from the dinosauria. In *The application of ichnology to palaeoenvironmental and stratigraphic analysis* (ed. D Mclroy), pp. 93–123. London, UK: Geological Society London Special Publication 228.
- Niedzwiedzki G, Szrek P, Narkiewicz K, Narkiewicz M, Ahlberg PE. 2010 Tetrapod trackways from the early middle Devonian period of Poland. *Nature* **463**, 43–48. (doi:10.1038/nature08623)
- DiMaggio JA, Vernon W. 2011 *Forensic podiatry: principles and methods*, p. 200. New York, NY: Springer.
- Kennedy RB. 2005 A large-scale statistical analysis of barefoot impressions. *J. Forensic Sci.* **50**, 200.
- Pataky TC, Mu T, Bosch K, Rosenbaum D, Goulermas JY. 2011 Gait recognition: highly unique dynamic plantar pressure patterns among individuals. *J. R. Soc. Interface* **9**, 790–800. (doi:10.1098/rsif.2011.0430)
- D'Aout K, Meert L, Van Gheluwe B, De Clercq D, Aerts P. 2010 Experimentally generated footprints in sand: analysis and consequences for the interpretation of fossil and forensic footprints. *Am. J. Phys. Anthropol.* **141**, 515–525. (doi:10.1002/ajpa.21169)
- Hitchcock E. 1858 *Ichnology of New England. A report on the sandstone of the Connecticut valley, especially its fossil footmarks*. Boston, MA: Wm. White.
- Hatala KG, Dingwall HL, Wunderlich RE, Richmond BR. 2012 An experimentally-based interpretation of 1.5 million-year-old fossil hominin footprints: implications of human foot function. *Am. J. Phys. Anthropol.* **147**(Suppl. 54), 161.
- Falkingham PL, Margetts L, Manning PL. 2010 Fossil vertebrate tracks as paleopenetrometers:

- confounding effects of foot morphology. *Palaios* **25**, 356–360. (doi:10.2110/palo.2009.p09-164r)
13. Falkingham PL, Bates KT, Margetts L, Manning PL. 2011 The ‘Goldilocks’ effect: preservation bias in vertebrate track assemblages. *J. R. Interface* **8**, 1142–1154. (doi:10.1098/rsif.2010.0634)
 14. Falkingham PL. 2012 Acquisition of high resolution 3D models using free, open-source, photogrammetric software. *Palaeo. Elect.* **15**, 1T:15p.
 15. Pataky TC, Goulermas JY, Crompton RH. 2008 A comparison of seven methods of within-subjects rigid body pedobarographic image registration. *J. Biomech.* **41**, 3085–3089. (doi:10.1016/j.jbiomech.2008.08.001)
 16. Pataky TC, Caravaggi P, Savage R, Parker D, Goulermas JY, Sellers WI, Crompton RH. 2008 New insights into the plantar pressure correlates of walking speed using pedobarographic statistical parametric mapping (pSPM). *J. Biomech.* **41**, 1987–1994. (doi:10.1016/j.jbiomech.2008.03.034)
 17. LeJeune TM, Willems PA, Heglund CE. 1998 Mechanics and energetics of human locomotion on sand. *J. Exp. Biol.* **201**, 2071–2080.
 18. Crevier-Denoix N, Robin D, Pourcelot P, Falala S, Holden P, Estoup P, Desquilbet L, Denoix JM, Chateau H. 2010 Ground reaction force and kinematic analysis of limb loading on two different beach sand tracks in harness trotters. *Equine Vet. J.* **38**, 544–551. (doi:10.1111/j.2042-3306.2010.00202.x)
 19. Raichlen DA, Gordon AD, Harcourt-Smith WEH, Foster AD, Randall Hass W. 2010 Laetoli footprints preserve earliest evidence of human-like bipedal biomechanics. *PLoS ONE* **5**, e9769. (doi:10.1371/journal.pone.0009769)